PHYSICAL REVIEW A VOLUME 5, NUMBER 4 APRIL 1972

Electron Transmission Spectroscopy: Rare Gases*

L. Sanche and G. J. Schulz
Department of Engineering and Applied Science Mason Laboratory, Yale University, New Haven, Connecticut 06520
(Received 10 November 1971)

A transmission experiment is used to observe structure in the total electron-impact cross section for He, Ne, Ar, Kr, and Xe below the respective ionization potentials, and also in the region of autoionizing states. The positions of the resonances are tabulated and compared with the results of other investigators. In both neon and argon, relatively large isolated resonances exist near the edge of the Rydberg series involving inner-shell autoionizing states, i.e., near 47.5 and 29 eV, respectively.

I. INTRODUCTION

This paper describes an experiment which detects structure in the total electron-impact cross section by a study of the unscattered current transmitted through a gas-filled collision chamber. This method, first introduced by Ramsauer and Kollath[1] for a measurement of the total electron-impact cross section was later refined by Kuyatt *et al.*,[2] by Golden and co-workers,[3,4] and by Schulz,[5] and used for a study of resonances in electron-atom scattering. In all these experiments, the unscattered transmitted current is measured as a function of electron energy and the structure of this curve is examined. The transmitted current for monoenergetic electrons is given by the relation $I(E) = I_0 e^{-NQ_tL}$, where I_0 is the current entering the collision chamber, $Q_t(E)$ is the total effective scattering cross section for electrons[2] of energy E, L is the path length, and N is the gas density. Previous experiments[2-5] have deduced the structure in the elastic cross section by measuring directly the transmitted current. We shall discuss below that many advantages accrue when the derivative of the transmitted current is measured directly, as we are doing in the present experiment. Another major advance over some previous experiments is the absence, in the present experiment, of electron optical focusing effects. This advantage arises from our use of an axial magnetic field to align the electrons. The only previous experiment[5] using an axial magnetic field suffered from relatively poor energy resolution and low signal-to-noise ratio. Both these problems are probably inherent in the use of the retarding-potential-difference method for producing "monochromatic" electrons. These deficiencies are overcome in the present experiment by using the trochoidal electron monochromator, which has recently been developed by Stamatovic and Schulz.[6] It is the only device now available that can give a narrow electron-energy distribution in the presence of the desired axial magnetic field.

As a result of the improvements in the technique, we are able to observe structures in the cross sections with a much higher signal-to-noise ratio than was possible previously. We are thus in a position to evaluate those structures which appeared only weakly in previous experiments and to reexamine conflicting observations, especially in the case of helium. For the remainder of the rare gases we are able to present a much more complete picture on the location of resonances than was previously possible.

We are correlating the observed structures with resonances in electron-atom scattering. However, experiments of this kind cannot detect resonances which are relatively broad, and other methods must be used if one wishes to observe such resonances. Methods to accomplish this have been developed for molecules where one can study dissociative attachment and its isotope effect, and vibrational excitation.

Sections II–IV of this paper discuss the methods used in the present experiment; Secs. V–VII discuss resonances in all the rare gases up to their respective ionization potentials; Secs. VIII–XI deal with higher energies, i.e., above the first ionization potential.

II. ELECTRON TRANSMISSION SPECTROMETER

The electron transmission spectrometer shown in Fig. 1 consists of a trochoidal monochromator followed by a collision chamber, retarding plates R, and a collector C. The principle of operation of the trochoidal monochromator has been previously described.[6] Electrons emitted from a thoriacoated iridium filament F are aligned by an axial magnetic field B of 130 G. The three electrodes following the filament have holes (1.0, 0.5, and 0.25 mm in diameter) drilled off-center by 1.6 mm. Thus, electrons enter the deflection region off-center. In this region a crossed electric and magnetic field is established by application of a small potential across two parallel surfaces (1.9 cm long and spaced 1.5 mm apart). Usually, the monochromator is operated with a voltage of 0.3 V between the par-

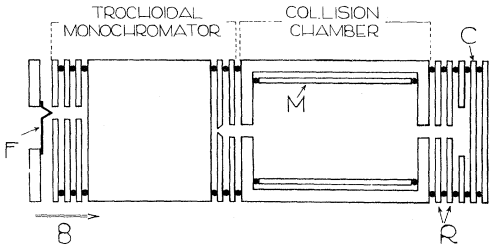

FIG. 1. Schematic diagram of apparatus.

allel surfaces. This produces an electron beam of about 5×10^{-9} A with an energy spread between 30 and 40 meV (full width at half-maximum). In the crossed-field region, the electrons describe a trochoidal motion and their guiding center moves with a velocity $\tilde{E}\times\tilde{B}/B^2$. Here, $\tilde{E}$ and $\tilde{B}$ are the electric and magnetic field intensities. Electrons are dispersed according to their axial velocities and those electrons which reach the center of the tube are transmitted through the exit hole of the monochromator which has a diameter of 0.5 mm and is located on-axis.

The monoenergetic electrons are accelerated into a collision chamber where they make collisions with the target gas. The pressure inside the collision chamber is about 0.03 torr. Those electrons which reach the exit of the collision chamber are decelerated to about 0.2 eV by two retarding electrodes R. This deceleration prevents most of the scattered electrons from reaching the electron collector C, because the scattered electrons have their velocity vector reoriented and thus do not possess sufficient axial momentum to overcome the potential barrier set by the two electrodes R. Inelastically scattered electrons are also unable to overcome this barrier. Thus, the energy selection and angular collimation achieved in this manner permit measurement of the unscattered portion of the electron beam (at the collector C). Since electron optical focusing effects can be minimized when the electron beam is magnetically aligned, the transmitted current is not falsified by these effects.

The apparatus is assembled using 1.5-mm sapphire balls as spacers between the different components of the tube. The electrodes, which are 2.5 cm in diameter and about 2 mm thick, have six equidistant holes drilled in them on a common circle to serve as seats for the sapphire balls. The two plates adjoining the electron collector serve as guard plates and are maintained at the collector potential. The tube is constructed of gold-plated Advance and molybdenum. The vacuum system is bakeable up to 350 °C and a liquid-nitrogen trap provides isolation from the 500-liter/sec oil diffusion pump.

III. DERIVATIVE TECHNIQUE

As shown in Fig. 1, an insulated cylinder M is inserted into the collision chamber. To this cylinder we apply a small alternating potential, 0.005–0.06 V, with respect to the entrance and exit electrodes of the collision chamber. The frequency is 730 Hz. This produces a modulation in the electron energy; the resulting modulation on the transmitted current (at the collector C) is detected synchronously using a synchronous (lock-in) detector. The output of this synchronous detector is applied to the Y axis of an X-Y recorder, whose X axis is driven by the ramp generator which controls the accelerating voltage. With a constant modulation voltage ΔE, we can write for the ac component of the transmitted current $\Delta I \propto \Delta I/\Delta E \simeq -I_0 NL(dQ_t/dE)e^{-NQ_tL}$. Many of the structures that we wish to study cause only small changes in Q_t; for these, the exponential term remains essentially constant over the region of a single resonance and to a first approximation the measured ac current ΔI is proportional to (dQ_t/dE). This quantity remains small until a sharp change in Q_t occurs. Hence, sharp variations in $I(E)$ can easily be identified as they stand out from a relatively flat background signal. In particular, sharp resonances can be identified since they produce at least one minimum and one maximum in the derivative curve.

The optimum value of the gas density which produces the largest modulated signal can be obtained from the above equation by setting its derivative (with respect to N) to zero. The result for this optimum is $NQ_tL = 1$, and in fact present experiments show that the largest signal is obtained near this gas density.

The advantages of taking the derivative of the transmitted current are many. The method focuses on *changes* in the cross section, i.e., just the aspect one is interested in when one wishes to detect sharp resonant behavior. By applying the modulation voltage only within the volume of the collision chamber, one *eliminates the spurious effects which can be caused near the entrance and exit slits. Thus surface effects as well as fringing effects near these slits become unimportant.* We were able to demonstrate that some spurious structure that we could observe in the transmitted current without modulation is eliminated by the modulation technique.

The modulation technique necessarily causes a broadening of the electron-energy distribution in the collision chamber. However, by keeping the modulation voltage as low as possible (0.005–0.06 V), we were not often limited by this broadening effect. Other energy broadening effects, such as broadening due to the finite energy resolution of the trochoidal monochromator and variation of the

contact potential along the path length ("internal broadening"),[5] seem to dominate. In the case of helium, Doppler broadening also contributes. The narrowest structures observed appear to have a separation between maximum and minimum in the derivative curve about 0.03–0.06 eV.

IV. ELECTRON-ENERGY-SCALE CALIBRATION

In the past few years, the $(1s2s^2)\,^2S$ resonance in helium has become a favorite point for calibrating electron-energy scales. The original work[7] on this resonance placed the position of the peak of the resonance at 19.30 ± 0.10 eV, and subsequently this value was remeasured by Kuyatt *et al.*[2] (19.31 ± 0.03 eV), by Golden and Bandel[3] (19.285 ± 0.025 eV) and by Golden and Zecca[8] (19.30 ± 0.01 eV). We have taken the opportunity and recalibrated the location of the ^2S resonance, using the three different procedures discussed below.

(i) We compare the resonance with the onset of excitation of the $2\,^3S$ state whose threshold energy (19.818 eV) is known to high accuracy from spectrocopic data.[9] Unfortunately, the threshold shape of the $2\,^3S$ excitation is complicated by structure in the elastic cross section[10] (Wigner cusp) which starts slightly below the onset of the inelastic cross section. Hence, proper calibration of the helium resonance demands a detailed theoretical study of the shape of the total scattering cross section in the threshold region with a precise knowledge of the shape of the cusp at threshold. Such a study has recently been initiated[11] and it provides us with a theoretical shape for the derivative of the transmitted current in the vicinity of the $2\,^3S$ threshold. The theoretical shape of the curve matches rather well the experimental curve and this matching procedure enables us to locate the point on our experimental curve which corresponds to the $2\,^3S$ threshold. This calibration procedure leads to a value of 19.35 ± 0.02 eV for the zero point in the derivative curve for the ^2S resonance. This point corresponds to the position of the peak of the ^2S resonance in a direct transmission experiment and to the minimum in the cross section.

(ii) The second method of calibration consists of comparing the position of the $1s2s^2$ resonance with the onset of the zeroth vibrational state of the $a\,^3\Pi$ electronic state at 6.01 eV in CO using a gas mixture of He and CO. Vibrational excitation of that state produces a series of well-defined dips in the derivatives of the transmitted current[12] whose width is only limited by the instrumental resolution. The $a\,^3\Pi$ state[12] of CO is therefore a reliable reference point. Calibration against that state gives 19.33 ± 0.02 eV for the helium resonance.

(iii) The third method uses a mixture of O_2 and He. We compare the position of the $1s2s^2$ resonance with the eighth vibrational level of the O_2^- $(^2\Pi_g)$ shape resonance. The energy of this level is known to an accuracy of ± 0.01 eV because of its coincidence with the third vibrational level of the O_2 electronic ground state.[13] The value we obtain using this procedure is 19.35 ± 0.02 eV.

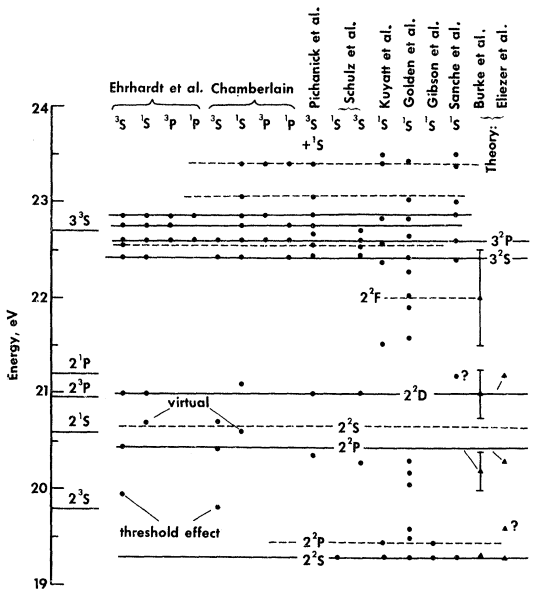

FIG. 2. Survey of the energy values for resonances in helium. The names of the authors are indicated, and also shown is the decay channel in which the resonances are observed. The heavy horizontal lines indicate the resonances which seem firmly established and the dashed lines indicate those that are still somewhat in doubt. See text for references.

All three calibrations agree within 20 meV, and we adopt the value 19.34 ± 0.02 eV for the $(1s2s^2)\,^2S$ state of He^-. The energy scales for the other rare gases are established by admixing a small amount of helium with the rare gas under investigation and comparing the position of the largest resonances in the rare gas with the helium resonance. We estimate the accuracy of the energy values in the other rare gases to be slightly less than in helium. For the first two resonances in each rare gas we estimate the absolute accuracy to be ± 0.03 eV and for the remainder of the structures, ± 0.05 eV.

V. HELIUM (19.3-25 eV)

Figure 2 shows in graphical form the location of resonances in helium, as observed in several decay channels by different authors. The data included are those of Ehrhardt and co-workers,[14,15] Chamberlain,[16] Pichanick *et al.*,[17] Schulz and Philbrick,[18] Kuyatt *et al.*,[2] Golden and Zecca,[8] Gibson and Dolder,[19] and the present data marked Sanche *et al.* Also included are the theories of Burke *et al.*[20] and of Eliezer and Pan.[21] The three low-lying resonances, namely, $2\,^2S$ (19.3 eV), $2\,^2P$ (20.4 eV), and

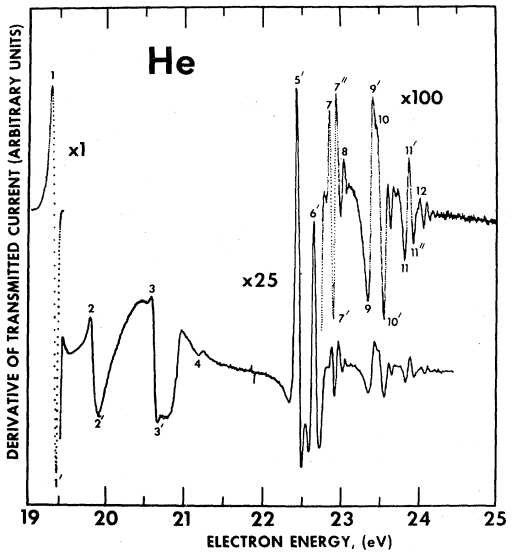

FIG. 3. Derivative of transmitted current vs electron energy in helium, below ionization. The gain of the amplifier is increased by a factor of 25 for the lower portion of the curve and by a factor of 100 for the inset in the upper right, compared to the region around 19.3 eV. The excursion around 19.3 eV corresponds to a change in transmitted current of about 10%. The smaller excursions (eg., No. 12) thus corresponds to a change in transmitted current of about 0.01%, which is the limit of the present experiment. All following figures have the same limitation.

2^2D (21.0 eV), are well established, and in fact angular distributions[14,15] for these states have been obtained. The 2^2P and 2^2D states are core-excited shape resonances and their preferred mode of decay leads to electronically excited states.

On the survey figure, there are listed two transmission experiments, that of Kuyatt *et al.*[2] and of Golden and Zecca,[4] in addition to the present one. Golden and Zecca find about twice as many structures in their curves compared to the results of Kuyatt *et al.* In fact, the impetus for the present experiment was given in part by this discrepancy, with the anticipation that with our larger sensitivity we would see the additional structure more clearly. As we shall discuss below, we are unable to find any structures in addition to those reported by Kuyatt *et al.* and thus we shall not give a detailed comparison with the data of Golden and Zeeca. In those instances where both Kuyatt *et al.* and Golden and Zecca observe structures, the agreement between the two experiments is good.

A plot of the derivative of the transmitted current versus electron energy obtained in the present experiment is shown in Fig. 3. Various features in Fig. 3 are numbered, and Table I gives the location of these features on the energy scale and a comparison with other experiments. The very large excursion near 19.3 eV is the $(1s2s^2)^2S$ resonance, which has been previously studied by various methods.

Some experiments in the literature show additional structure close to the $1s2s^2$ resonance, between 19.42 and 19.52 eV. We have examined this range of energy very carefully since it is important to establish whether this is actually the $(1s2s2p)^2P$ state, as postulated by Kuyatt *et al.*[2] and further studied by Gibson and Dolder.[19] In most of our runs we have been unable to observe any kind of structure around 19.50 eV, but when we were able

TABLE I. Position of resonances in helium (eV).

Feature number	Transmission experiments: Sanche and Schulz (present work)	Transmission experiments: Kuyatt *et al.* (Ref. 2)	Metastable production: Pichanick and Simpson (Ref. 17)	Differential: Ehrhardt and co-workers (Refs. 14 and 15)	Designation
1–1′	19.30–19.37	19.31–19.37			$2\,^2S$
		19.43–19.47			
2–2′	19.80–19.90	19.818			Wigner cusp $+2\,^3S$
			20.34	20.45	$2\,^2P$
3–3′	20.58–20.62	20.59			Wigner cusp $+2\,^1S$
			20.99	21.00	$2\,^2D$
4	21.19				
		21.50–21.55			
5–5′–5″	22.34–22.42–22.50	22.34–22.39	22.44	22.42	$3\,^2S$
6–6′–6″	22.60–22.65–22.73	22.54–22.60	22.55/22.67	22.55/22.60	$3\,^2P$
7–7′–7″	22.88–22.92–22.97	22.81–22.85	22.75/22.86	22.75/22.85	
8	23.05		23.05		
9–9′	23.35–23.43	23.30–23.44	23.39		$n=4$
10–10′	23.48–23.55	23.49			
11–11′–11″	23.82–23.88–23.93	23.75–23.82			$n=5$
12	24.03				

to bring in structure around 19.5 eV by artificially detuning the apparatus, the structure behaved in a most peculiar manner: We were able to make the feature move on the energy scale and disappear completely by altering the potential distribution near the entrance and exit of the collision chamber. The identical alterations in potential left all other resonances in their exact relative positions. Thus we consider the structure around 19.5 to be spurious, probably caused by effects near the entrance and exit electrodes of the collision chamber. Although we do not have definite proof, we believe that this structure is an "echo" of the $1s2s^2$ resonance. Electrons may lose a discrete amount of energy (~0.2 eV) by a collision with a gas-covered surface, and when this small group of electrons is accelerated by an additional 0.2 eV, it will replicate the structure of the $1s2s^2$ resonance.

The structure in the energy range 19.6–21.0 eV could result from various causes. Generally, this structure is interpreted as the depletion of the transmitted current by inelastic collisions. In order to test this hypothesis, we compare the derivative of the transmitted current obtained in the present experiment with a compatible curve which is derived from the "total metastable cross section" measured by Pichanick and Simpson.[17] This is shown in Fig. 4. The two curves are normalized to each other by adjusting the magnitude of the excursion just above the threshold of the 2^1S state. A comparison of the two curves of Fig. 4 shows deviations near 20 eV and a dramatic deviation in the vicinity of the 2^3S threshold. The deviation around 20 eV is not too

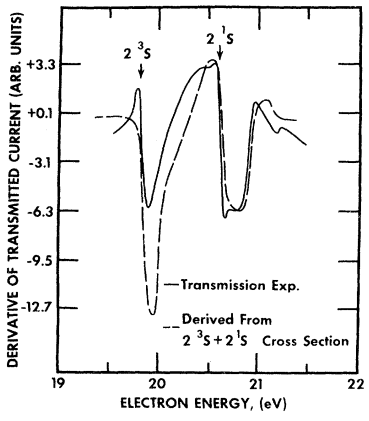

FIG. 4. An expanded view of the derivative of the transmitted current in the neighborhood of the lowest inelastic thresholds in helium. The solid line shows the present experiment and the dashed line is obtained from the total metastable cross section. The two curves are normalized to each other in the region of the $2\,^1S$ excitation. The rise in the transmission curve just below the threshold for the $2\,^3S$ state is interpreted as a Wigner cusp in the elastic cross section.

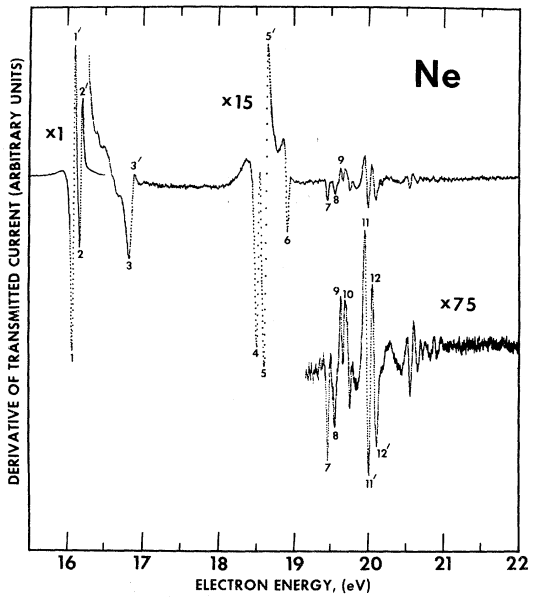

FIG. 5. Derivative of the transmitted current vs electron energy in neon. The expansion of the sensitivity is indicated. The energy positions of the numbered features are indicated in Table II.

surprising in view of the different nature of the experiments involved and the sensitive test we demand by plotting the derivative. In order for the two curves to agree fully one would have to be sure that the two experiments are performed using the same shape of the electron-energy distribution; that the secondary emission coefficient for electrons is the same for 2^3S and 2^1S metastables; and that no structure exists in the *elastic* cross section. Since none of the above conditions is assured, we cannot attach much significance to the deviation around 20 eV.

The deviation of the two curves of Fig. 4 which occurs just near 19.8 eV, i.e., near the threshold of the 2^3S state, appears to be significant. Here, our experimental derivative curve exhibits a rise, whereas the derivative of the transmitted current, when one considers inelastic processes, must necessarily decrease. In fact, the rise just below the threshold for the 2^3S state is impossible to explain on the basis of inelastic processes. Thus we must postulate that this rise is characteristic of the elastic cross section just below the 2^3S threshold. Such a behavior (Wigner cusp) has been postulated theoretically,[10] but not clearly identified experimentally. An analogous rise just below the energy of the 2^1S state can be interpreted similarly.

The structure observed in helium above 20 eV is compared with the experiments of Ehrhardt *et al.*[14,15] (differential inelastic cross section) and the experiments of Pichanick and Simpson[17] (total metastable production) in Table I. We also list the values obtained by Kuyatt *et al.*[2] in a transmission

TABLE II. Position of resonances in neon (eV).

Feature number	Transmission experiments: Sanche and Schulz (present work)	Transmission experiments: Kuyatt *et al.* (Ref. 2)	Metastable production: Pichanick and Simpson (Ref. 17)	Designation
1–1′	16.10–16.12	16.04		$(2p^5 3s^2)\ ^2P_{3/2}$
2–2′	16.19–16.22	16.135		$(2p^5 3s^2)\ ^2P_{1/2}$
3–3′	16.85–16.91		16.92	
...	...	18.18		
...	...	18.29		
4	18.55	18.46	18.35–18.43	
5–5′	18.65–18.70	18.56	18.58–18.66	
6	18.95		18.86–18.97	
7	19.47			
8	19.57			
9	19.65			
10	19.71		19.69	
11–11′	19.97–20.03		19.83	
12–12′	20.07–20.13		20.1	

experiment. The agreement is seen to be very good. A detailed designation beyond that given in the table is not as yet available.

VI. NEON (16-22 eV)

Our results in neon are shown in Fig. 5 and in Table II, where again comparison is made between other experimental determinations. The first two structures marked 1–1′ and 2–2′ have already been identified by Kuyatt *et al.*[2] as being the $(1s^2 2s^2 2p^5 3s^2)\ ^2P_{3/2,1/2}$ states of Ne^-. We confirm the splitting found by Kuyatt *et al.* Our value for this splitting, 95 ± 2 meV, is in exact agreement with that found by Kuyatt *et al.*, and it agrees with the spectroscopic value for the splitting found for the Ne^+ ion core (97 meV).

At higher energies, we find many clearly identified structures, not seen by Kuyatt *et al.* Interestingly, we do not find two structures observed (albeit very weakly) by Kuyatt *et al.* at 18.18 and at 18.29 eV, although our sensitivity appears to be much larger. Also, we do not find clearly developed inelastic thresholds. The resonantlike structure 3–3′ occurs at 16.85–16.91 eV and thus appears (possibly accidentally) coincident with the $^1P_1$ state at 16.848 eV. One may speculate that this is possibly the $2p^5 3s 3p$ state of Ne^-. It should be noted that the total excitation function for metastable states[17] shows a pronounced peak at 16.92 eV and we postulate that the threshold behavior of the electronic states is strongly influenced, possibly dominated, by the 16.85-eV resonance. The theoretical calculations of the ^1P excitation function for Ne by Sawada *et al.*[22] in fact show a sharp rise near threshold, which they attribute to a resonance.

A large energy gap occurs above 16.85 eV and the next resonance at 18.55 eV may be associated with the $2p^5 3p$ states of neon. Sharpton *et al.*[23] have observed a spike in the optical excitation function of the $2p^5 3p$ states at 18.6 eV. Probably this spike results from one of the compound states observed in the present experiment at 18.55 or 18.65

TABLE III. Position of resonances in argon (eV).

Feature number	Transmission experiments: Sanche and Schulz (present work)	Transmission experiments: Kuyatt *et al.* (Ref. 2)	Metastable production: Pichanick and Simpson (Ref. 17)	Designation
1–1′	11.10–11.13	11.064–11.094		$(3p^5 4s^2)\ ^2P_{3/2}$
2–2′	11.27–11.30	11.235–11.267		$^2P_{1/2}$
3	11.71		11.72	
4	11.91		11.88–11.98	
5–5′	12.89–12.92		12.80–12.93	
6–6′–6″	12.95–13.06–13.11		13.08	
7–7′	13.22–13.28		13.17–13.24	
8	13.33		13.37	
9–9′	13.45–13.50		13.55	
10–10′–10″	14.03–14.07–14.10			

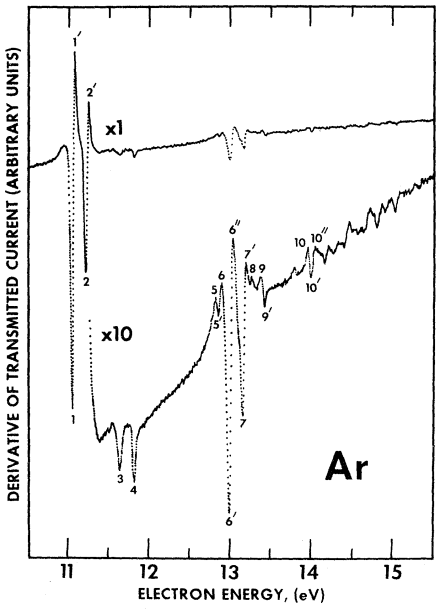

FIG. 6. Derivative of transmitted current vs electron energy in argon.

eV. We also remark that the splitting of the above two resonances is close to the splitting of the ion core. Surprisingly, the 16.85- and 18.95-eV resonances do not have such a companion.

VII. ARGON, KRYPTON, AND XENON BELOW IONIZATION

Our results in Ar, Kr, and Xe are shown in Figs. 6–8, and the values for the observed structures are listed in Tables III–V. In all these atoms, the two lowest-lying resonances are associated with the first excited states of the respective atom, and they show a splitting characteristic of the corresponding positive ion. The observed splittings are compared with the splittings of the ions in Table VI.

In argon, the structures observed at 11.71 and 11.91 eV (marked 3 and 4 in Fig. 6) could be interpreted as the $3p^5 4s4p$ states of Ar^-. The separation between these two levels is close to the ion splitting. The excitation function for Ar metastables[17] shows structure in the neighborhood of these resonances (at 11.72 and 11.9 eV). Also, one should note that the separation between the large resonances marked 6′ and 7 in Fig. 6 is close to the ion splitting. These are probably resonances associated with the higher-lying excited states of argon, obtained by adding $4p$ or $3d$ electrons to the $^2P_{3/2,1/2}$ ion core.

In krypton, the splitting of the two lowest resonances is so large (0.66 eV) that the upper of these resonances ($^2P_{1/2}$) lies above the two lowest triplet states ($^3P_2$, $^3P_1$) of Kr. Nevertheless, the resonance does not seem to be appreciably broadened; this would suggest that decay of the $^2P_{1/2}$ resonance to the $^3P_2$ and $^3P_1$ states is not large.

In fact, Swanson, Cooper, and Kuyatt[24] study the threshold behavior of the excitation to the $^3P_2$ and $^3P_1$ states and they find, for 90° scattering, that the $^2P_{1/2}$ resonance strongly enhances the excitation function to the $^3P_1$ state. Only a weak effect exists in the excitation function of the $^3P_2$ state. Swanson *et al.* also point out that the total angular momentum of the core has to change from $\frac{1}{2}$ to $\frac{3}{2}$ in this decay process and that this effect is analogous to Auger emission. Evidently, in krypton the decay involving

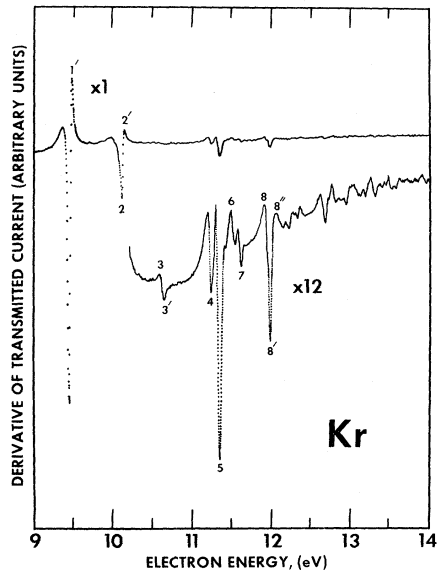

FIG. 7. Derivative of transmitted current vs electron energy in krypton.

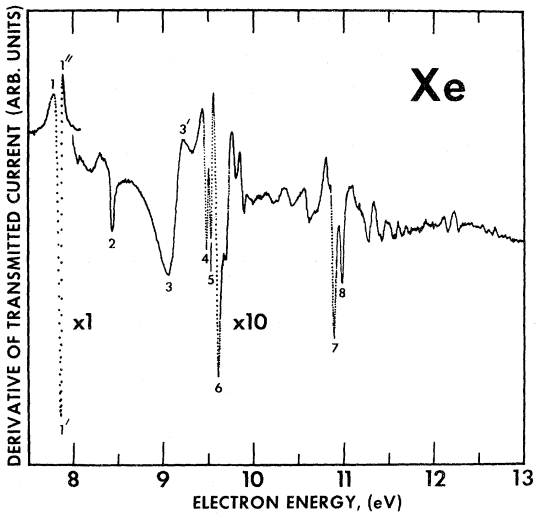

FIG. 8. Derivative of transmitted current vs electron energy in xenon.

TABLE IV. Position of resonances in krypton (eV).

Feature number	Transmission experiments: Sanche and Schulz (present work)	Transmission experiments: Kuyatt *et al.* (Ref. 2)	Metastable production: Pichanick and Simpson (Ref. 17)	Designation
1–1′	9.50–9.53	9.45–9.48		$(4p^5 5s^2)\,^2P_{3/2}$
2–2′	10.16–10.19	10.10	10.05	$^2P_{1/2}$
3–3′	10.66–10.69		10.63	
4	11.29		11.10–11.20	
5	11.40			
6	11.54		11.48	
7	11.67		11.70	
8–8′–8″	11.97–12.04–12.10		11.94–12.04	
			12.28	
			13.08	

emission of an s-wave electron (leading to the $^3P_1$ final state) is favored over the emission of a d-wave electron (leading to the $^3P_2$ final state). As in the case of the other rare gases, the ion splitting is reproduced at higher energies, namely, in the splitting of the large resonances marked 5 and 8′ in Fig. 7.

In xenon, where the core splitting is even larger (1.2 eV) than in krypton, the upper resonance $^2P_{1/2}$ is considerably broadened. Strangely, a resonant structure seems to lie between the $^2P_{3/2}$ and the $^2P_{1/2}$ states, at 8.48 eV. The large structures marked 6 and 7 in Fig. 8 are separated by the value of the ion splitting in xenon. We also note that structure is observed above the ionization limit of Xe. Such resonances can decay, by two-electron emission to form Xe^+ and can be sometimes observed as structure in the ionization curve. This type of decay is discussed, for the case of helium, in Sec. VIII.

VIII. HELIUM (57-59 eV)

Helium is known to have two compound states above the first ionization continuum. These states have been previously observed in transmission experiments[2,8] and identified[25] as the $(2s^2 2p)\,^2P$ and $(2s2p^2)\,^2D$ states. They can decay by the emission of a single electron[26] into various excited states of He (e.g., $2\,^3S$, $2\,^1S$, $2\,^1P$) and by the emission of two electrons into He^+. The latter decay has been discovered from observations using the trapped-electron method.[27] It is to be expected that the two-electron decay of these He^- states causes an interference effect in the production of He^+, and this structure in the He^+ production has been discovered by Grissom, Comtpon, and Garrett.[28] Recently, the structure in the He^+ formation has been studied with remarkable sensitivity by Quéméner, Paquet, and Marmet[29] and the interference structure resulting from the $2s^2 2p$ and $2s2p^2$ states (at 57.15 and 58.23 eV, respectively) has been clearly identified and the line shapes analyzed. Further structures at higher energies, resulting from doubly excited autoionizing states of neutral helium have also been observed by these authors.

Our own results for the derivative of the transmitted current versus electron energy are shown in Fig. 9, which exhibits the two He^- states. The zero value of the derivatives occurs at 57.16 ± 0.05 and 58.25 ± 0.05 eV, respectively. The calibration for these values is obtained from the $1s2s^2$ resonance in helium at 19.34 eV. The values we obtain

TABLE V. Position of resonances in xenon (eV).

Feature number	Transmission experiments: Sanche and Schulz (present work)	Transmission experiments: Kuyatt *et al.* (Ref. 2)	Metastable production: Pichanick and Simpson (Ref. 17)	Designation
1–1′–1″	7.80–7.90–7.92	7.74–7.77		$(5p^5 6s^2)\,^2P_{3/2}$
2	8.48			
3–3′	9.11–9.26	9.02	9.0	$^2P_{1/2}$
4	9.52			
5	9.56		9.5	
6	9.65			
7	10.92	10.81–10.86	10.3	
8	11.00			

TABLE VI. Comparison of $^2P_{3/2}$–$^2P_{1/2}$ splitting.

Gas	Compound state: Sanche and Schulz (present work)	Kuyatt *et al.* (Ref. 2)	Ion (Ref. 2)
Ne	0.095	0.095	0.097
Ar	0.172	0.172	0.177
Kr	0.66	0.64	0.666
Xe	~1.2	1.25	1.306

are in excellent agreement with the values of Quéméner *et al.* (57.15 ± 0.04 and 58.23 ± 0.04 eV) which were obtained by referring the resonant structure of He^+ to the ionization threshold. Also, previous determinations[2] are in good agreement with the latest values quoted above.

We also observe structure at higher energies, near 59.9 and 62.9 eV. These structures are about one hundred times smaller than the resonance at 57.16 eV, and they correspond to the structures found by Quéméner *et al.*,[29] who interpret these structures as doubly excited states. Trapped-electron studies[28] also show structure in this energy range.

IX. NEON (42-50 eV)

Figure 10 shows our results for neon, and Table VII gives the energies for the main features of Fig. 10. For comparison, we also show in Table VII the results of the trapped-electron method[30] and the main inelastic processes observed by electron impact at 90-eV energy.[31] We shall discuss the features of Fig. 10 starting at the lowest energy.

(a) 42 eV: This feature has been observed also by Grissom *et al.*[30] and by Marmet.[32] If the position of the $2s^22p^4\ (^3P)3s^2\ (^3P)$ state is really at the position calculated[30,33] by Weiss (42.18 eV), then the 42.0-eV features could be a resonance associated with this state. But the designation remains uncertain.

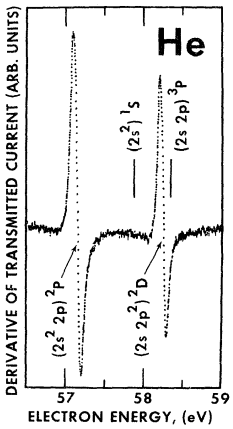

FIG. 9. Derivative of transmitted current vs electron energy at higher energies in helium.

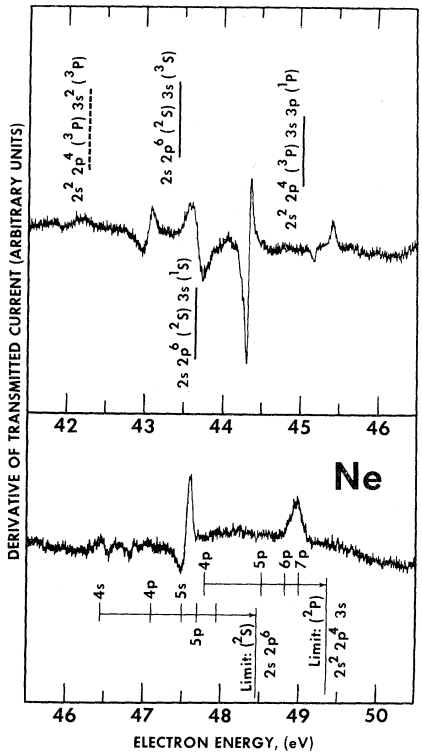

FIG. 10. Derivative of transmitted current vs electron energy at higher energies in neon.

(b) 43.0 eV: We consider this feature a resonance associated with the $2s2p^63s\ ^3S$ and ^1S states of neon which are located[33] at 43.28 and 43.64 eV. The shape shown in Fig. 10 strongly favors this assignment.

(c) 43.6 eV: This feature coincides in energy with a large inelastic loss peak ($2s2p^63s$) observed by Simpson *et al.*[31] The shape shown in Fig. 10 is probably characteristic of an inelastic threshold which is coupled to the continuum.

(d) 44.3 eV: This feature is an unmistakable

TABLE VII. Features in neon (41–50 eV).

Sanche and Schulz (present work) (transmission)	Grissom *et al.* (Ref. 30) (trapped electrons)	Simpson (Ref. 31) (inelastic)	Possible designation
41.98	42.1	···	resonance
43.00–43.11	···	···	resonance
43.61–43.73	···	43.6	inelastic
44.33–44.38	44.0–44.51	···	resonance
45.18		45.0	
45.43	45.53	45.6	
46.58		46.5	
46.86	46.8		
		47.1	
47.53–47.63	47.57		resonance
		47.7	
49.03			step
	49.86		

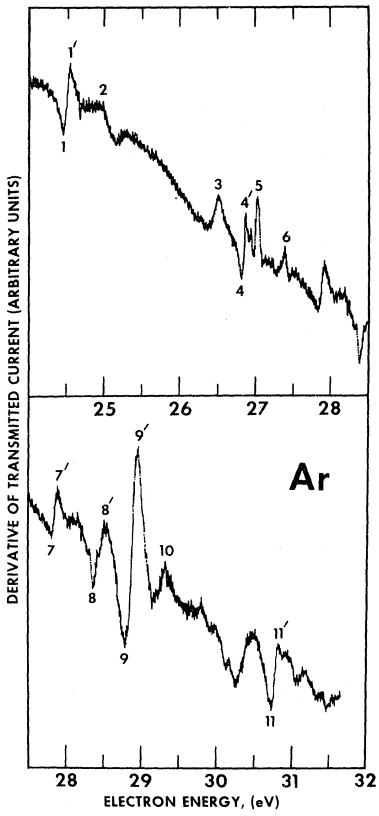

FIG. 11. Derivative of transmitted current vs electron energy at higher energies in argon.

resonance, probably having the $2s^2 2p^4 3s3p$ state as a parent. In the trapped-electron method,[30] and in ion production,[32] this feature appears much broader than in the present experiment where it is limited by our energy resolution.

The subsequent features in the energy range 44.5–47 eV are small and we are not able to provide an interpretation.

(e) 47.5 eV: The feature at 47.5–47.6 eV has the shape of a resonance. We find it surprising that an isolated resonance occurs in an energy region where innumerable excited states exist. This feature certainly deserves some elucidation by theory.

(f) 49.0 eV: The feature at 49.0 eV is a clear "hump," indicating that a step has occurred in the cross section. A feature in the Ne^+ spectrum lies at the same energy.[32] Again we find the pronounced isolated feature at such high energies surprising. The series limit $(2s^2 2p^4 3s)\,^2P$ lies at 49.37 eV.

X. ARGON (24-32 eV)

Figure 11 shows a plot of the derivative of the transmitted current versus electron energy in argon between 24 and 32 eV. Table VIII lists the energies of the features observed in the present experiments and compares the location of the features with structure recently observed in the positive-ion cross section.[34] Also, we list in Table VIII the inelastic processes observed in the energy range of interest and some possible designations. The justification for some of the designations, principally features 1, 2, and 6 has been provided by Bolduc *et al.*[34] The results of other experiments[35–37] are also presented in Table VIII.

The lowest identified autoionizing states in argon are the $3s3p^6 4s$ states[34,35] at 24.96 and 25.22 eV. Following the arguments of Bolduc *et al.*,[34] it is reasonable to associate the structure 1–1′ in Fig. 11 with a resonance having a configuration of $(3s3p^6 4s^2)\,^2S$.

Further structure is listed in Table VIII. The

TABLE VIII. Features in argon (24–31 eV). Note: The "possible designation" of features 1, 2, and 6 has been taken from the work of Bolduc, Quéméner, and Marmet (Ref. 34).

Feature number	Sanche and Schulz [a] (transmission)	Bolduc *et al.* [b] (ionization)	Other authors	Simpson *et al.* [c] (inelastic)	Possible designation
1–1′	24.48–24.58	24.44			$(3s3p^6 4s^2)\,^2S$
2	25.03	24.96			$(3s3p^6 4s)\,^3S$
		25.25	25.22 [d]	25.2	^1S
3	26.55	26.60	26.62 [e]	26.72	$(3s3p^6 4p)\,^1P$
4–4′	26.84–26.90				resonance
5	27.07				
6	27.41	27.43			$(3s3p^6 3d)\,^3D$
		27.61	27.57 [f]	27.55	^1D
7–7′	27.87–27.95				resonance
8–8′	28.41–28.58				
9–9′	28.82–28.98				resonance
10	29.36				
11–11′	30.75–30.86				

[a] Present work.
[b] See Ref. 34.
[c] See Ref. 31.
[d] See Ref. 35.
[e] See Ref. 36.
[f] See Ref. 37.

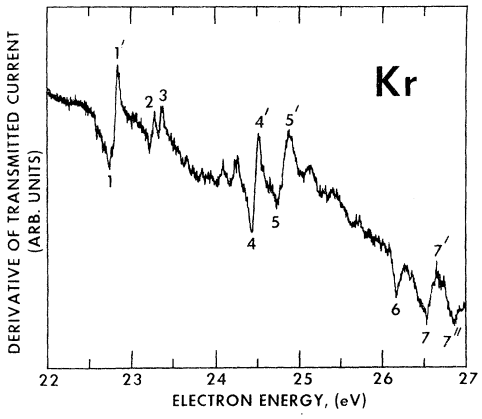

FIG. 12. Derivative of transmitted current vs electron energy at higher energies in krypton.

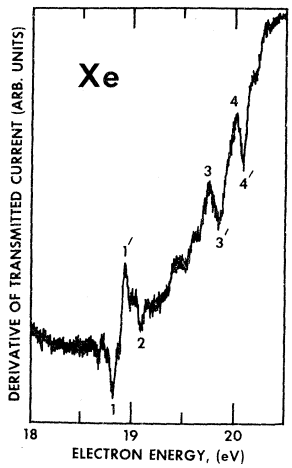

FIG. 13. Derivative of transmitted current vs electron energy at higher energies in xenon.

features 4–4′ and 7–7′ are most probably resonances, since these features are sharp and do not coincide with any known autoionizing states.[31]

As in the case of neon, we note that a relatively large resonantlike structure (marked 9–9′ in Fig. 11) exists in a sea of autoionizing states, near 29 eV, i.e., close to the edge of the Rydberg series. This phenomenon, possibly associated with collective oscillations, bears further investigation. No dominant inelastic process involving an energy loss near 29 eV has been observed by Simpson *et al.*,[31] or by Brion and Olsen.[37] Thus we can exclude the possibility that the 29-eV process is inelastic.

XI. KRYPTON (22-27 eV) and XENON (18-20 eV)

Energy levels for krypton and xenon in the region of autoionizing states have not been the subject of extensive investigations, and thus a detailed analysis of Figs. 12 and 13 cannot be presented. The lowest identified states in this energy range have been listed by Bergmark *et al.*[35] They place the $4s4p^6 5s$ state of krypton at 23.73 eV and the $5s5p^6 6s$ state of xenon at 20.08 eV. Our first structure in each gas lies about 1 eV below these states, and we propose that these structures are resonances. The designation is probably $4s4p^6 5s^2$ for krypton and $5s5p^6 6s^2$ for xenon. Other resonant structures, shown in Figs. 12 and 13, are listed in Tables IX and X.

XII. CONCLUSIONS

The transmission method described in this paper has yielded a more complete survey of resonances in the rare gases than was available to date. Whereas the resonances observed near the lowest electronically excited states of the neutral atom are amenable to an interpretation, the higher resonances can only be listed, as was the case with spectral lines in the early days of optical spectroscopy. Nevertheless, such a listing is of interest because collision phenomena cannot be completely understood without a knowledge of the position of resonances. Missing from this survey are very short-lived resonances ($\lesssim 10^{-15}$ sec). Such resonances are also important for collision problems, but they appear broad and are not readily studied by the methods of this paper.

When one analyzes resonances above the first ionization potential, one is faced with a multitude of autoionizing parent states, and interpretation in all gases except helium becomes very tenuous. It is surprising to us that in this sea of excited states, some resonances in neon and argon appear so prominently and are isolated. This observation merits the attention of theorists.

The method of observation presented in this paper is suitable for similar work in molecules. In the case of diatomic molecules (O_2 and NO), it appears that the more prominent structures occur in the form of vibrational progressions.[38] These vibrational progressions are associated with Rydberg states of molecules, as evidenced by the spacing and the Franck-Condon factors of the vibrational progressions. This circumstance makes identifica-

TABLE IX. Features in krypton (22–27 eV).

1–1′	2	3	4–4′	5–5′	6	7–7′–7″
22.76–22.87	23.30	23.39	24.46–24.54	24.78–24.91	26.18	26.56–26.68–26.90

TABLE X. Features in xenon (18–20 eV).

1–1′	2	3–3′	4–4′
18.85–18.96	19.13	19.78–19.88	20.10–20.17

tion of resonances, in specific cases, easier in diatomic molecules than in atoms.

ACKNOWLEDGMENTS

We are indebted to A. Herzenberg for frequent discussions and for elucidation of many theoretical problems and to P. Marmet for showing us his ionization data before publication. Also, thanks are due P. D. Burrow and J. C. Steelhammer for their comments and advice.

*Work supported by the U. S. National Science Foundation.

[1]For a review, see H. S. W. Massey and E. H. S. Burhop, *Electronic and Ionic Impact Phenomena* (Clarendon, Oxford, 1969), Vol. I.

[2]C. E. Kuyatt, J. A. Simpson, and S. R. Mielczarek, Phys. Rev. 138, A385 (1965).

[3]D. E. Golden and H. W. Bandel, Phys. Rev. 38, A14 (1965).

[4]D. E. Golden and A. Zecca, Phys. Rev. A 1, 241 (1970).

[5]G. J. Schulz, Phys. Rev. 136, A650 (1964).

[6]A. Stamatovic and G. J. Schulz, Rev. Sci. Instr. 41, 423 (1970).

[7]G. J. Schulz, Phys. Rev. Letters 10, 104 (1963).

[8]D. E. Golden and A. Zecca, Phys. Rev. A 1, 241 (1970).

[9]C. E. Moore, *Atomic Energy Levels*, Natl. Bur. Std. (U. S.) Circ. No. 467 (U. S. GPO, Washington, D. C. 1958), Vol. III.

[10]E. P. Wigner, Phys. Rev. 73, 1002 (1948); A. I. Baz, Zh. Eksperim. i Teor. Fiz. 33, 923 (1957) [Sov. Phys. JETP 6, 709 (1958)].

[11]Ton That Dinh and A. Herzenberg (private communication).

[12]L. Sanche and G. J. Schulz, Phys. Rev. Letters 26, 943 (1971). The spectroscopic values for the $a\,^3\Phi$ state of CO are listed in R. W. B. Pearse and A. G. Gaydon, *The Indentification of Molecular Spectra* (Chapman and Hall, London, 1965).

[13](a) D. Spence and G. J. Schulz [Phys. Rev. A 2, 1802 (1970)] find an accidental coincidence between the $v=8$ vibrational level of O_2^- and the $v=3$ level of O_2. (b) This observation has recently been confirmed by F. Linder and H. Schmidt, in *Abstracts of the Seventh International Conference on the Physics of Electronic and Atomic Collisions, Amsterdam*, 1971 (North-Holland, Amsterdam, 1971), p. 336.

[14]H. Ehrhardt and K. Willmann, Z. Physik 203, 1 (1967).

[15]H. Ehrhardt, L. Langhans, and F. Linder, Z. Physik 214, 179 (1968).

[16]G. E. Chamberlain, Phys. Rev. 155, 46 (1967).

[17]F. M. J. Pichanick and J. A. Simpson, Phys. Rev. 168, 64 (1968).

[18]G. J. Schulz and J. W. Philbrick, Phys. Rev. Letters 13, 477 (1964).

[19]J. R. Gibson and K. T. Dolder, J. Phys. B 2, 741 (1969).

[20]P. G. Burke, J. W. Cooper, and S. Ormond, Phys. Rev. 183, 245 (1969).

[21]I. Eliezer and Y. K. Pan, Theoret. Chem. Acta (Berlin) 16, 63 (1970).

[22]T. Sawada, J. E. Purcell, and A. E. S. Green, Phys. Rev. A 4, 193 (1971).

[23]F. A. Sharpton, R. M. St. John, C. C. Lin, and F. E. Fajen, Phys. Rev. A 2, 1305 (1970).

[24]N. Swanson, J. W. Cooper, and C. E. Kuyatt, in Ref. 13(b), p. 323.

[25]U. Fano and J. W. Cooper, Phys. Rev. 138, A400 (1965).

[26]J. A. Simpson, M. G. Menendez, and S. R. Mielczarek, Phys. Rev. 150, 76 (1966).

[27]P. D. Burrow and G. J. Schulz, Phys. Rev. Letters 22, 1271 (1969).

[28]J. T. Grissom, R. N. Compton, and W. R. Garrett, Phys. Letters 30A, 117 (1969).

[29]J. J. Quéméner, C. Paquet, and P. Marmet, Phys. Rev. A 4, 494 (1971).

[30]J. T. Grissom, W. R. Garrett, and R. N. Compton, Phys. Rev. Letters 23, 1011 (1969).

[31]J. A. Simpson, S. R. Mielczarek, and J. Cooper, J. Opt. Soc. Am. 54, 269 (1964).

[32]P. Marmet (private communication).

[33]A. Weiss (private communication).

[34]E. Bolduc, J. J. Quéméner, and P. Marmet, Can. J. Phys. (to be published).

[35]T. Bergmark, R. Spohr, N. Magnusson, L. O. Werme, C. Nordling, and K. Siegbahn, Uppsala University Institute of Physics Report No. 589, 1969 (unpublished).

[36]R. P. Madden, D. L. Ederer, and K. Codling, Phys. Rev. 177, 136 (1969).

[37]C. E. Brion and L. A. R. Olsen, J. Phys. B 3, 1020 (1970).

[38]L. Sanche and G. J. Schulz, Phys. Rev. Letters 27, 1333 (1971).